Katholieke Universiteit Leuven

Departement Elektrotechniek

ESAT-SISTA/TR 08-10

A First-Order Frequency-Warped Sigma Delta Modulator with Improved Signal-to-Noise Ratio[1]

Ludovico Ausiello[2] [3], Toon van Waterschoot[4], and Marc Moonen[5]

August 2008
Published in *Proceedings of the 16th European Signal Processing Conference (EUSIPCO '08)*, Lausanne Switzerland, Aug. 2008.

[1]This report is available by anonymous ftp from *ftp.esat.kuleuven.be* in the directory *pub/sista/vanwaterschoot/reports/08-10.pdf*

[2]ARCES, University of Bologna, Via Toffano 2, 40125 Bologna, Italy, Tel. +39 051 2095400, Fax +39 051 2095410, WWW: *http://www.arces.unibo.it*. E-mail: *lausiello@arces.unibo.it*.

[3]This research work was carried out at the ESAT laboratory of the Katholieke Universiteit Leuven, in the frame of the Edith Program, the Belgian Programme on Interuniversity Attraction Poles, initiated by the Belgian Federal Science Policy Office IUAP P6/04 (DYSCO, 'Dynamical systems, control and optimization', 2007-2011), and EU/FP7-ICT-2007-1 Project 216785 ("Ultra-wide band real-time interference monitoring and cellular management strategies – UCELLS"), and was supported by the Marie Curie Early Stage Training No. 504125 and the Institute for the Promotion of Innovation through Science and Technology in Flanders (IWT-Vlaanderen). The scientific responsibility is assumed by its authors.

[4]K.U.Leuven, Dept. of Electrical Engineering (ESAT), Research group SCD(SISTA), Kasteelpark Arenberg 10, 3001 Leuven, Belgium, Tel. +32 16 321927, Fax +32 16 321970, WWW: *http://homes.esat.kuleuven.be/∼tvanwate*. E-mail: *toon.vanwaterschoot@esat.kuleuven.be*.

[5]K.U.Leuven, Dept. of Electrical Engineering (ESAT), Research group SCD(SISTA), Kasteelpark Arenberg 10, 3001 Leuven, Belgium, Tel. +32 16 321060, Fax +32 16 321970, WWW: *http://www.esat.kuleuven.be/scd*. E-mail: *marc.moonen@esat.kuleuven.be*.

16th European Signal Processing Conference (EUSIPCO 2008), Lausanne, Switzerland, August 25-29, 2008, copyright by EURASIP

A FIRST-ORDER FREQUENCY-WARPED SIGMA DELTA MODULATOR WITH IMPROVED SIGNAL-TO-NOISE RATIO

Ludovico Ausiello[1], *Toon van Waterschoot*[2], *and Marc Moonen*[2]

[1]ARCES, University of Bologna
Via Toffano 2, 40125 Bologna, Italy
phone: +39 051 2095400, fax: +39 051 2095410
email: lausiello@arces.unibo.it
web: www.arces.unibo.it

[2]ESAT-SCD, Katholieke Universiteit Leuven
Kasteelpark Arenberg 10, B-3001 Leuven, Belgium
phone: +32 16 321709, fax: +32 16 321970
email: {tvanwate,moonen}@esat.kuleuven.be
web: www.esat.kuleuven.be/scd

ABSTRACT

A design procedure for first-order oversampling sigma delta modulators (SDM) is proposed, which incorporates a particular frequency warping. By warping the SDM noise transfer function with positive warping parameters, the out-of-band gain can be decreased and hence stability properties can be improved. Moreover, an appropriate choice of the corresponding warped SDM loop filters leads to a signal transfer function that provides a boost in the signal band, thereby yielding an increase in signal-to-noise ratio (SNR). This paper describes the design procedure and SNR analysis for two different first-order frequency-warped SDM topologies, which require only one additional multiplier compared to the traditional SDM structure. The most promising one of these topologies is compared with the traditional first-order SDM in computer simulations using sinusoidal test signals, and yields an SNR improvement of 6 dB.

1. INTRODUCTION

A Sigma Delta Modulator (SDM) is a non-linear device widely used in analog-to-digital (A/D) conversion to achieve a high resolution without requiring high-precision analog components. Its typical output stream has two fundamental characteristics, namely a few-bit word representing the amplitude of the incoming signal and a very high symbol rate. A high signal-to-noise ratio (SNR) can be obtained by increasing the oversampling ratio (OSR) and by decreasing the noise power in the band of interest using specific filter topologies [1],[2]. As seen in Fig. 1, the building blocks of the system are a low-pass filter (integrator), an A/D convertor (comprising a sample-and-hold circuit and a quantizer), and a negative feedback loop including a reconstructor for digital-to-analog (D/A) conversion. The usual linear model for the quantizer (which actually makes the system non-linear) is an additive noise source and a gain. The noise source represents the quantization noise, introduced by the low-bit quantizer. First-order SDMs are particularly interesting because of their well-understood stability properties and low complexity [3],[4].

We can think of the whole SDM as a device in which the feedback signal represents the quantization noise, while the low-pass filter in the feedforward path is designed to cancel it and to process its frequency content, moving it to a part of the spectrum that is not important for the specific application. For example, in audio A/D conversion, the quantization noise is shifted to a frequency interval that is higher than the audio band. A properly designed low-pass filter is thus needed to achieve the desired performance in terms of SNR and signal-to-noise-and-distortion ratio (SINAD). With the intent of increasing the performance of a SDM without affecting the complexity of the low-pass filter, a design procedure for SDMs is proposed, which incorporates a particular frequency warping [5]. The resulting SDM is expected to achieve a better SNR and SINAD compared to a traditional topology of the same order, due to an increased frequency selectivity of the warped modulator filter.

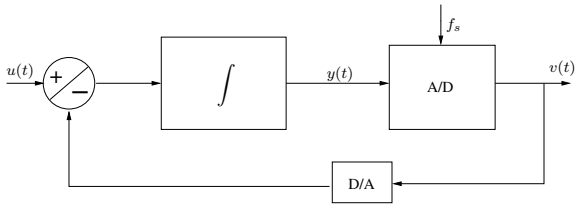

Figure 1: Block diagram for a Sigma Delta Modulator.

As already proposed in lossy audio coding techniques [6], a non-uniform representation of the frequency axis can be an instrumental for increasing the frequency resolution in the low part of the spectrum, emulating the human cochlear behaviour that approximately has a constant-Q analysis capability [7]. By embedding this feature directly into the SDM, we can expect a better performance because of the more selective noise shaping. In audio applications, it is usually preferred to combine a high symbol rate (e.g., high oversampling ratio (OSR)) with relatively simple low-pass filters, made up of only one or two integrator stages. We propose a procedure for designing first-order frequency-warped SDM architectures that have two distinct advantages over the traditional first-order SDM: a lower noise transfer function (NTF) Nyquist gain (also called "out-of-band gain"), which is important for stability issues [3], and a signal transfer function (STF) that is shaped to be more frequency selective, hence improving the SNR performance. These advantages can be achieved without changing the complexity of the filter in a drastic manner. Frequency warping of higher-order SDMs, which are of importance in A/D conversion problems where the applicable OSR is limited due to the large signal bandwidth, e.g. in telecommunications, is considered in [8].

This paper is organized as follows. In Section 2 we present the design procedure for obtaining first-order frequency-warped SDMs. Depending on how the frequency warping is chosen to affect the STF, two different first-order topologies are derived, which require only one additional multiplier compared to the traditional first-order SDM structure. In Section 3, we perform a SNR analysis for these first-order frequency-warped SDM topologies and for different types of input signals. Finally, in Section 4, we present some simulation results of first-order frequency-warped SDMs and compare them to traditional SDMs in terms of SNR. Section 5 concludes the paper.

This research work was carried out at the ESAT laboratory of the Katholieke Universiteit Leuven, in the frame of the Edith Program and the Belgian Programme on Interuniversity Attraction Poles, initiated by the Belgian Federal Science Policy Office IUAP P6/04 (DYSCO, 'Dynamical systems, control and optimization', 2007-2011) and was supported by the Marie Curie Early Stage Training No. 504125 and the Institute for the Promotion of Innovation through Science and Technology in Flanders (IWT-Vlaanderen). The scientific responsibility is assumed by its authors.

2. FIRST-ORDER FREQUENCY-WARPED SDM DESIGN

2.1 Notation

The notation used throughout this paper is adopted from [3]. We can represent a SDM as a two-input, single-output device as depicted in Fig. 2. The A/D quantizer is denoted by Q and modeled as an additive noise source and a gain, while the A/D sample-and-hold circuit and the D/A reconstructor are assumed to be complementary and are hence not included in the model. In the following, $G(z)$ denotes the STF and $H(z)$ the NTF. $U(z)$ is the input signal and $V(z)$ is the encoded output. If we define the error signal as $E(z) = V(z) - Y(z)$, we can present the classical input-output relation for the modulator, that is

$$V(z) = G(z)U(z) + H(z)E(z) \tag{1}$$

and the so-called loop filters are defined as

$$L_0(z) = \frac{Y(z)}{U(z)} = \frac{G(z)}{H(z)} \tag{2}$$

and

$$L_1(z) = \frac{Y(z)}{V(z)} = \frac{H(z)-1}{H(z)}. \tag{3}$$

It is important to remember that in this simplified linear model the noise is signal-dependent.

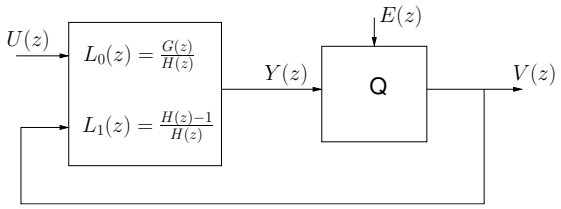

Figure 2: General block diagram of a single-quantizer SDM.

2.2 Design Procedure: Derivation

The simplest first-order noise shaping function is a pure differentiator, having a transfer function

$$H(z) = 1 - z^{-1}. \tag{4}$$

The NTF can be warped by replacing the complex variable z with the bilinear all-pass function $\frac{z-\lambda}{1-\lambda z}$ (or, equivalently, by replacing z^{-1} with $\frac{z^{-1}-\lambda}{1-\lambda z^{-1}}$) [5], leading to

$$H(z,\lambda) = 1 - \frac{z^{-1}-\lambda}{1-\lambda z^{-1}} = \frac{(1+\lambda)(1-z^{-1})}{1-\lambda z^{-1}}. \tag{5}$$

As pointed out in [3], the NTF should always be scaled such that the first tap of its impulse response is 1. This is necessary to assure that the L_1 loop filter contains at least one pure time delay, hence avoiding an algebraic loop in the closed-loop SDM scheme. The first tap of the impulse response of $H(z,\lambda)$ equals $(1+\lambda)$, hence the desired warped and scaled NTF is obtained by dividing the transfer function in (5) by $(1+\lambda)$,

$$\boxed{\tilde{H}(z,\lambda) = \frac{1-z^{-1}}{1-\lambda z^{-1}}.} \tag{6}$$

The magnitude response of $\tilde{H}(z,\lambda)$ is shown in Figs. 3(a) and 3(b) for positive and negative warping parameters, respectively.

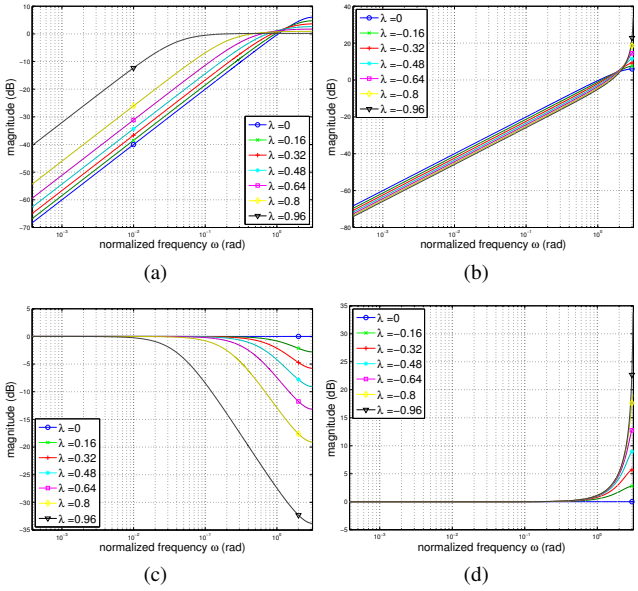

Figure 3: First-order frequency-warped SDM: (a) NTF magnitude response ($\lambda \geq 0$), (b) NTF magnitude response ($\lambda \leq 0$), (c) STF magnitude response, (topology I, $\lambda \geq 0$), (d) STF magnitude response (topology I, $\lambda \leq 0$).

The corresponding warped loop filter $\tilde{L}_1(z,\lambda)$ can then be calculated as follows:

$$\tilde{L}_1(z,\lambda) = \frac{\tilde{H}(z,\lambda)-1}{\tilde{H}(z,\lambda)} = -(1-\lambda)\frac{z^{-1}}{1-z^{-1}}. \tag{7}$$

At this point the warped SDM design allows for some freedom in deciding how the frequency warping will affect the STF $G(z)$. The effect on $G(z)$ follows directly from the choice of the loop filter $\tilde{L}_0(z,\lambda)$. A first possibility is to constrain the warped loop filters $\tilde{L}_0(z,\lambda)$ and $\tilde{L}_1(z,\lambda)$ to obey the same relationship as in the non-warped case, i.e.,

$$L_0(z) = -L_1(z) \Rightarrow \tilde{L}_0(z,\lambda) = -\tilde{L}_1(z,\lambda). \tag{8}$$

This choice leads to

$$\tilde{L}_{0,1}(z,\lambda) = (1-\lambda)\frac{z^{-1}}{1-z^{-1}} \tag{9}$$

which corresponds to the first-order SDM topology shown in Fig. 4, denoted as topology I. It can be seen that the warping merely comes down to adding a gain factor $(1-\lambda)$ in the SDM forward path. The warped STF $\tilde{G}_1(z,\lambda)$ is in this case given by

$$\boxed{\tilde{G}_1(z,\lambda) = (1-\lambda)\frac{z^{-1}}{1-\lambda z^{-1}}} \tag{10}$$

which is a high-pass filter if $\lambda < 0$, a low-pass filter if $\lambda > 0$, and a pure time delay if $\lambda = 0$. The STF magnitude response is plotted in Figs. 3(c) and 3(d) for positive and negative warping parameters, respectively. In audio applications, the positive range of the warping parameter is more interesting, because of the intention of emulating the cochlear frequency resolution behaviour. Furthermore, a positive value of λ yields a low-pass STF, even in the first-order case (while in the non-warped case $G(z) = z^{-1}$ has a flat STF frequency response). Finally, for positive warping parameters, the NTF frequency response has smaller out-of-band gain (see Figs. 3(a)), which is beneficial for SDM stability [3].

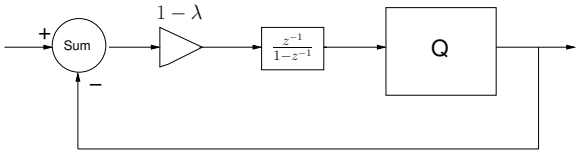

Figure 4: First-order frequency-warped SDM topology I ($\tilde{L}_0(z,\lambda) = -\tilde{L}_1(z,\lambda)$).

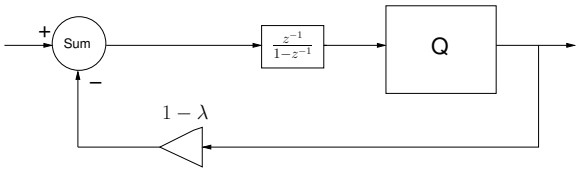

Figure 5: First-order frequency-warped SDM topology II ($\tilde{L}_0(z,\lambda) = L_0(z)$).

A second possibility for completing the design of the first-order warped SDM is to constrain $\tilde{L}_0(z,\lambda)$ to be equal to the loop filter $L_0(z)$ in the non-warped first-order SDM, i.e.,

$$\tilde{L}_{0,\mathrm{II}}(z,\lambda) = \frac{z^{-1}}{1-z^{-1}} \tag{11}$$

which leads to

$$\boxed{\tilde{G}_{\mathrm{II}}(z,\lambda) = \frac{z^{-1}}{1-\lambda z^{-1}}.} \tag{12}$$

The resulting topology, denoted as topology II, is shown in Fig. 5, and only differs from topology I in the position of the gain factor $(1-\lambda)$, which is now in the feedback path. Obviously, the NTF $\tilde{H}(z,\lambda)$ is the same for both topologies, whereas the STF $\tilde{G}_{\mathrm{II}}(z,\lambda)$ is a scaled version of the STF $\tilde{G}_{\mathrm{I}}(z,\lambda)$ in (10), the scaling being such that the gain at dc increases for increasing λ, whereas for topology I it is equal to 0 dB for all values of λ. This can be seen from the topology II STF magnitude response, plotted in Figs. 6(a) and 6(b) for positive and negative values of λ, respectively.

We should mention that, while the warped and scaled first-order NTF in (6) can be considered as a special case of the NTF of the so-called enhanced first-order SDM [4], the STFs proposed in (10) and (12) are not special cases of the STF in [4], due to the absence of a delay in the SDM feedback path. As a consequence, the results on SNR and the stability analysis presented in [4], cannot be applied to the proposed first-order frequency-warped SDM topologies.

The implementation of the proposed first-order frequency warped SDM topologies only requires an additional multiplier compared to the traditional implementation, either in the forward path or in the feedback path, hence the increase in computational complexity or hardware cost is limited. The equivalent C-code for implementing both the traditional and the frequency-warped modulator filters can be found in [8]. We should note that, in this simple first-order design example, the frequency warping effect is not fully exploited. The zero of the non-warped NTF in (4) is at dc, a frequency that is always mapped onto itself under the frequency transform associated with the bilinear frequency warping. As a consequence, the frequency warping can in this case only affect the radius of the NTF zero, and not its angle. Apart from a radial displacement of the zero, the frequency warping also adds a (real) pole at $z = \lambda$ to the NTF (and also to the STF in both topologies considered above).

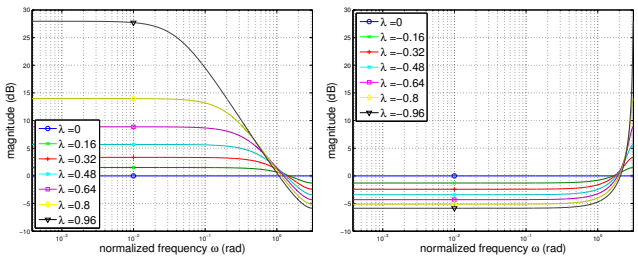

(a) (b)

Figure 6: First-order frequency-warped SDM: (a) STF magnitude response (topology II, $\lambda \geq 0$), (b) STF magnitude response (topology II, $\lambda \leq 0$).

3. SNR ANALYSIS

The SNR of the first-order frequency-warped SDM topologies described above can be predicted using the analytical SDM model presented in Section 2.1. The SNR is defined as the ratio of the power of the input signal component in the output signal and the power of the quantization noise component in the output signal,

$$\mathrm{SNR} = 10\log_{10}\frac{\sigma_{xv}^2}{\sigma_{ev}^2} \tag{13}$$

which are calculated in the signal band $[0, f_B]$, with f_B the input signal bandwidth, see e.g. [4],

$$\sigma_{xv}^2 = \int_0^{f_B} |\tilde{G}(f,\lambda)|^2 |X(f)|^2 df \tag{14}$$

$$\sigma_{ev}^2 = \int_0^{f_B} |\tilde{H}(f,\lambda)|^2 |E(f)|^2 df. \tag{15}$$

Using the fact that $2f_B = f_S/\mathrm{OSR}$, with f_S the sampling frequency and OSR the oversampling ratio, the integrals in (14) and (15) can be written in terms of the normalized radial frequency variable $\omega = 2\pi f/f_S$,

$$\sigma_{xv}^2 = \frac{f_S}{2\pi}\int_0^{\pi/\mathrm{OSR}} |\tilde{G}(\omega,\lambda)|^2 |X(\omega)|^2 d\omega \tag{16}$$

$$\sigma_{ev}^2 = \frac{f_S}{2\pi}\int_0^{\pi/\mathrm{OSR}} |\tilde{H}(\omega,\lambda)|^2 |E(\omega)|^2 d\omega. \tag{17}$$

First of all, we evaluate σ_{ev}^2, assuming that the quantization noise $E(z)$ has a flat power spectrum in the signal band $[0, f_B]$ (cfr. [4]), i.e., $|E(\omega)|^2 = \sigma_e^2$, $\forall \omega \in [0, \pi/\mathrm{OSR}]$. Under this assumption, (17) can be rewritten as

$$\sigma_{ev}^2 = \frac{f_S \sigma_e^2}{2\pi}\int_0^{\pi/\mathrm{OSR}} |\tilde{H}(\omega,\lambda)|^2 d\omega. \tag{18}$$

The magnitude response of the first-order warped and scaled NTF in (6) can be calculated as follows,

$$|\tilde{H}(\omega,\lambda)|^2 = \left|\frac{1-e^{-j\omega}}{1-\lambda e^{-j\omega}}\right|^2 \tag{19}$$

$$= 2\frac{1-\cos\omega}{1-2\lambda\cos\omega+\lambda^2} \tag{20}$$

hence

$$\sigma_{ev}^2 = \frac{f_S \sigma_e^2}{\pi}\int_0^{\pi/\mathrm{OSR}} \frac{1-\cos\omega}{1-2\lambda\cos\omega+\lambda^2} d\omega. \tag{21}$$

If $\lambda \neq 0$, using the substitution $t = \tan\frac{\omega}{2}$ (implying that $\cos\omega = \frac{1-t^2}{1+t^2}$ and $d\omega = \frac{2dt}{1+t^2}$), and subsequently applying a partial fraction

expansion, the integral in (21) can be rewritten as follows,

$$\int \frac{1-\cos\omega}{1-2\lambda\cos\omega+\lambda^2}d\omega = \int \frac{4t^2}{(1+t^2)[(1-\lambda)^2+(1+\lambda)^2t^2]}dt$$
$$= \frac{1}{\lambda}\left[\int \frac{dt}{1+t^2} - \frac{(1-\lambda)^2}{(1+\lambda)^2}\int \frac{dt}{\frac{(1-\lambda)^2}{(1+\lambda)^2}+t^2}\right] \quad (22)$$
$$= \frac{1}{\lambda}\left[\arctan t - \frac{1-\lambda}{1+\lambda}\arctan\Big(\frac{1+\lambda}{1-\lambda}t\Big)\right] \quad (23)$$
$$= \frac{1}{\lambda}\left[\frac{\omega}{2} - \frac{1-\lambda}{1+\lambda}\arctan\Big(\frac{1+\lambda}{1-\lambda}\tan\frac{\omega}{2}\Big)\right]. \quad (24)$$

If $\lambda = 0$, the integral in (21) reduces to

$$\int (1-\cos\omega)d\omega = \omega - \sin\omega. \quad (25)$$

Substituting (24) and (25) in (21) yields

$$\boxed{\sigma_{ev}^2 = \frac{f_S\sigma_e^2}{\pi\lambda}\left[\frac{\pi}{2\mathrm{OSR}} - \frac{1-\lambda}{1+\lambda}\arctan\Big(\frac{1+\lambda}{1-\lambda}\tan\frac{\pi}{2\mathrm{OSR}}\Big)\right]} \quad (26)$$

for $\lambda \neq 0$ and

$$\sigma_{ev}^2 = \frac{f_S\sigma_e^2}{\pi}\Big(\frac{\pi}{\mathrm{OSR}} - \sin\frac{\pi}{\mathrm{OSR}}\Big) \quad (27)$$

for $\lambda = 0$. Using de l'Hôpital's rule, it can be shown that

$$\lim_{\lambda\to 0}\frac{f_S\sigma_e^2}{\pi\lambda}\left[\frac{\pi}{2\mathrm{OSR}} - \frac{1-\lambda}{1+\lambda}\arctan\Big(\frac{1+\lambda}{1-\lambda}\tan\frac{\pi}{2\mathrm{OSR}}\Big)\right] \quad (28)$$
$$= \frac{f_S\sigma_e^2}{\pi}\Big(\frac{\pi}{\mathrm{OSR}} - \sin\frac{\pi}{\mathrm{OSR}}\Big) \quad (29)$$

such that the set of equations in (27)-(26) defines a continuous function of $\lambda \in (-1,1)$.

Subsequently, we evaluate σ_{xv}^2 for both warped SDM topologies I and II. An important difference with the SNR analysis for the traditional first-order SDM, which has a flat STF frequency response, is that we have to assume knowledge of the input signal power spectrum $|X(\omega)|^2$ for evaluating (16) when $\lambda \neq 0$. We will consider two extreme cases, the input signal being either a white noise (WN) signal or a pure sinusoidal tone (SIN). The behavior of the predicted SNR as a function of λ will show to be very similar in both cases, hence we can expect a similar SNR behavior for more realistic non-white, broadband signals. Before evaluating the power of the input signal component in the SDM output signal $V(z)$ according to (16), we calculate the STF magnitude response for the warped SDM topology I defined by (10),

$$|\tilde{G}_{\mathrm{I}}(\omega,\lambda)|^2 = \left|\frac{(1-\lambda)e^{-j\omega}}{1-\lambda e^{-j\omega}}\right|^2 \quad (30)$$
$$= \frac{(1-\lambda)^2}{1-2\lambda\cos\omega+\lambda^2} \quad (31)$$

and likewise for topology II, defined by (12),

$$|\tilde{G}_{\mathrm{II}}(\omega,\lambda)|^2 = \frac{1}{1-2\lambda\cos\omega+\lambda^2}. \quad (32)$$

If we assume that the input signal is a WN signal with variance σ_x^2, then (16) can be rewritten as

$$\sigma_{xv,\mathrm{I}}^2 = \frac{f_S\sigma_x^2}{2\pi}(1-\lambda)^2\int_0^{\pi/\mathrm{OSR}}\frac{d\omega}{1-2\lambda\cos\omega+\lambda^2} \quad (33)$$
$$\sigma_{xv,\mathrm{II}}^2 = \frac{f_S\sigma_x^2}{2\pi}\int_0^{\pi/\mathrm{OSR}}\frac{d\omega}{1-2\lambda\cos\omega+\lambda^2} \quad (34)$$

for topologies I and II, respectively. Performing the substitution $t = \tan\frac{\omega}{2}$ allows us to solve the integral in (33)-(34) as follows:

$$\int \frac{d\omega}{1-2\lambda\cos\omega+\lambda^2} = \frac{2}{(1+\lambda)^2}\int \frac{dt}{\frac{(1-\lambda)^2}{(1+\lambda)^2}+t^2} \quad (35)$$
$$= \frac{2}{(1+\lambda)^2}\frac{1+\lambda}{1-\lambda}\arctan\Big(\frac{1+\lambda}{1-\lambda}t\Big) \quad (36)$$
$$= \frac{2}{(1+\lambda)(1-\lambda)}\arctan\Big(\frac{1+\lambda}{1-\lambda}\tan\frac{\omega}{2}\Big)$$

which leads to

$$\boxed{\begin{aligned}\sigma_{xv,\mathrm{I}}^2 &= \frac{f_S\sigma_x^2}{\pi}\frac{1-\lambda}{1+\lambda}\arctan\Big(\frac{1+\lambda}{1-\lambda}\tan\frac{\pi}{2\mathrm{OSR}}\Big)\\ \sigma_{xv,\mathrm{II}}^2 &= \frac{f_S\sigma_x^2}{\pi}\frac{1}{1-\lambda^2}\arctan\Big(\frac{1+\lambda}{1-\lambda}\tan\frac{\pi}{2\mathrm{OSR}}\Big).\end{aligned}} \quad (37)$$

On the other hand, if we assume the input signal to be a pure sinusoidal tone with power σ_x^2 and radial frequency $\omega_0 \in [0,\pi/\mathrm{OSR}]$,

$$|X(\omega)|^2 = \frac{\sigma_x^2}{2}\left[\delta(\omega+\omega_0)+\delta(\omega-\omega_0)\right] \quad (38)$$

then (16) can be calculated as follows, using the fact that $|\tilde{G}(\omega_0,\lambda)|^2 = |\tilde{G}(-\omega_0,\lambda)|^2$:

$$\sigma_{xv}^2 = \frac{f_S\sigma_x^2}{2\pi}\int_0^{\pi/\mathrm{OSR}}|\tilde{G}(\omega_0,\lambda)|^2 d\omega \quad (39)$$
$$= \frac{f_S\sigma_x^2}{2\pi}|\tilde{G}(\omega_0,\lambda)|^2\frac{\pi}{\mathrm{OSR}} \quad (40)$$
$$= \sigma_x^2 f_B|\tilde{G}(\omega_0,\lambda)|^2 \quad (41)$$

which leads to

$$\boxed{\begin{aligned}\sigma_{xv,\mathrm{I}}^2 &= \frac{\sigma_x^2 f_B(1-\lambda)^2}{1-2\lambda\cos\omega_0+\lambda^2}\\ \sigma_{xv,\mathrm{II}}^2 &= \frac{\sigma_x^2 f_B}{1-2\lambda\cos\omega_0+\lambda^2}.\end{aligned}} \quad (42)$$

As a result, for $\lambda \neq 0$, the predicted SNR using the analytical model for the first-order frequency-warped SDM can be obtained using (26), (37), and (42), for topologies I and II, and in case of WN and SIN input signals, respectively:

$$\boxed{\begin{aligned}\mathrm{SNR}_{\mathrm{I}}(\mathrm{WN}) &= 10\log_{10}\frac{\sigma_x^2}{\sigma_e^2}\lambda\frac{1-\lambda}{1+\lambda}\Gamma(\lambda)\\ \mathrm{SNR}_{\mathrm{II}}(\mathrm{WN}) &= 10\log_{10}\frac{\sigma_x^2}{\sigma_e^2}\frac{\lambda}{1-\lambda^2}\Gamma(\lambda)\end{aligned}} \quad (43)$$

$$\boxed{\begin{aligned}\mathrm{SNR}_{\mathrm{I}}(\mathrm{SIN}) &= 10\log_{10}\frac{\sigma_x^2}{\sigma_e^2}\lambda\frac{(1-\lambda)^2}{1-2\lambda\cos\omega_0+\lambda^2}\Phi(\lambda)\\ \mathrm{SNR}_{\mathrm{II}}(\mathrm{SIN}) &= 10\log_{10}\frac{\sigma_x^2}{\sigma_e^2}\frac{\lambda}{1-2\lambda\cos\omega_0+\lambda^2}\Phi(\lambda)\end{aligned}} \quad (44)$$

with

$$\Gamma(\lambda) = \frac{\arctan\big(\frac{1+\lambda}{1-\lambda}\tan\frac{\pi}{2\mathrm{OSR}}\big)}{\frac{\pi}{2\mathrm{OSR}} - \frac{1-\lambda}{1+\lambda}\arctan\big(\frac{1+\lambda}{1-\lambda}\tan\frac{\pi}{2\mathrm{OSR}}\big)} \quad (45)$$
$$\Phi(\lambda) = \frac{1}{1-\frac{2\mathrm{OSR}}{\pi}\frac{1-\lambda}{1+\lambda}\arctan\big(\frac{1+\lambda}{1-\lambda}\tan\frac{\pi}{2\mathrm{OSR}}\big)}. \quad (46)$$

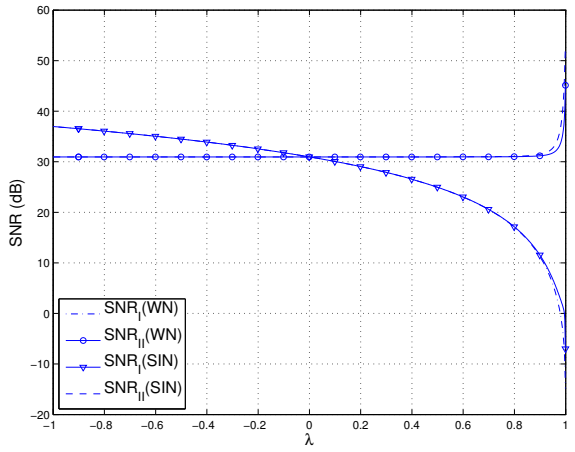

Figure 7: Predicted SNR vs. warping parameter for first-order frequency-warped SDM topologies I and II (WN = White noise input, SIN = sinusoidal input).

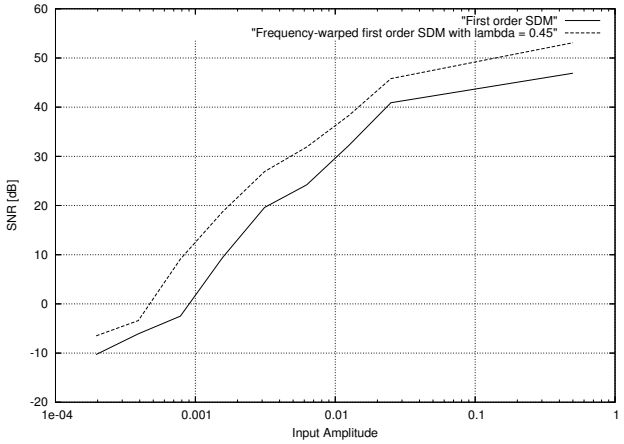

Figure 8: SNR comparison between a first-order traditional SDM and frequency-warped SDM (topology II) for $\lambda = 0.45$.

The SNR expressions for $\lambda = 0$ can equivalently be obtained using (27), (37), and (42).

The predicted SNR is plotted versus the warping parameter $\lambda \in (-1,1)$ in Fig. 7 for $\sigma_x^2/\sigma_e^2 = 1$, OSR $= 64$, $f_B = 24$ kHz, and $f_0 = 1$ kHz (such that $\omega_0 = (f_0/f_B)(\pi/\text{OSR}) = 2.0453e-3$ rad). For both signal types, we observe that the SNR of topology I decreases dramatically as $\lambda \to 1$, while it rises somewhat as $\lambda \to -1$. On the other hand, the SNR of topology II is predicted to increase strongly for $\lambda \to 1$, while it remains more or less constant for other values of λ. This behavior could be expected by examining the NTF and STF magnitude responses in Figs. 3 and 6. The warped NTF magnitude response rises significantly in the signal band at high OSRs when $\lambda \to 1$ (e.g., for $\lambda = 0.8$, the NTF magnitude response is 10 dB higher compared to the non-warped NTF response if $\omega < 3 \cdot 10^{-1}$ rad, corresponding to the entire signal band for OSRs larger than 10, see Fig. 3(a)). On the other hand, the STF magnitude response remains constant or even decreases (for positive λ) within the signal band for the warped SDM topology I, see Fig. 3(c), which obviously leads to a loss of SNR. In contrast, the STF magnitude response of topology II shows a boost in the signal band, which increases as $\lambda \to 1$, and which (over)compensates for the increase in the NTF response, see Fig. 6(a). From this analysis, we expect the positive range of the warping parameter to be most promising in terms of SNR improvement. This observation will be confirmed by simulation results in Section 4.

4. SIMULATION RESULTS

The positive range $[0,1)$ of the warping parameter λ is of particular interest for first-order frequency-warped SDMs, since it renders the frequency warping perceptually relevant in audio applications [6],[7], and since it yields frequency-warped SDMs of which the NTF frequency response has smaller out-of-band gain (see Fig. 3(a)), which is beneficial for SDM stability [3]. In Section 3, it was shown that the SNR is expected to increase for positive λ only when topology II is used.

After implementing the first-order frequency-warped SDM topology II in C-code, extensive simulations of more than $3 \cdot 10^6$ samples were run with sinusoidal input signals of variable amplitude, and with $f_0 = 1kHz$. The signal bandwidth was $f_B = 24kHz$ and the OSR $= 64$, resulting in a sampling frequency $f_S = 3072$ kHz. The plot representing the SNR for both the traditional SDM and the frequency-warped one is shown in Fig. 8. For several positive values of the warping parameter λ we have found better results in the SNR performance indicator as compared to the traditional SDM, with an optimum average 6 dB gain for $\lambda = 0.45$.

5. CONCLUSION

In this paper, we have incorporated frequency warping into the design of first-order SDMs, to obtain two first-order frequency-warped SDM topologies. It was observed that the NTF out-of-band gain decreases as the warping parameter goes to unity, which is beneficial to SDM stability. An SNR analysis was performed for sinusoidal and WN input signals, and it was conluded that, for positive warping parameters, the proposed topology II is most promising in terms of SNR improvement. The predicted SNR improvement was confirmed by simulation results with sinusoidal test signals.

REFERENCES

[1] J. Candy and G. Temes, Eds., *Oversampling Delta-Sigma Data Converters: Theory, Design, and Simulation*. Piscataway, NJ: IEEE Press, 1992.

[2] P. M. Aziz, H. V. Sorensen, and J. van der Spiegel, "An overview of sigma-delta converters," *IEEE Signal Process. Mag.*, vol. 13, no. 1, pp. 61–84, Jan. 1996.

[3] R. W. Adams and R. Schreier, "Stability theory for ΔΣ modulators," in *Delta-Sigma Data Converters: Theory, Design, and Simulation*, S. R. Norsworthy, R. Schreier, and G. C. Temes, Eds. Piscataway, NJ: IEEE Press, 1997, ch. 4.

[4] M. A. Al-Alaoui and R. Ferzli, "An enhanced first-order sigma-delta modulator with a controllable signal-to-noise ratio," *IEEE Trans. Circuits Syst.*, vol. 53, no. 3, pp. 634–643, Mar. 2006.

[5] A. V. Oppenheim, D. H. Johnson, and K. Steiglitz, "Computation of spectra with unequal resolution using the fast Fourier transform," *Proc. IEEE*, vol. 59, no. 2, pp. 299–301, Feb. 1971.

[6] A. Härmä and U. K. Laine, "A comparison of warped and conventional linear predictive coding," *IEEE Trans. Speech Audio Process.*, vol. 9, no. 5, pp. 579–588, July 2001.

[7] J. O. Smith and J. S. Abel, "Bark and ERB bilinear transforms," *IEEE Trans. Speech Audio Process.*, vol. 7, no. 6, pp. 697–708, Nov. 1999.

[8] L. Ausiello, T. van Waterschoot, and M. Moonen, "Design and evaluation of frequency-warped sigma delta modulators," submitted for publication in *IEEE Trans. Signal Process.* ESAT-SISTA Technical Report TR 07-190, Katholieke Universiteit Leuven, Belgium, Apr. 2008. [Online]. Available: ftp://ftp.esat.kuleuven.be/pub/sista/vanwaterschoot/abstracts/07-190.html